MAX-PLANCK-INSTITUT FÜR PLASMAPHYSIK

GARCHING BEI MÜNCHEN

Alternative Constraints in the Entropy Principle for Tokamak Profiles Applied to Cylindrical Plasmas

D. Pfirsch , F. Pohl

IPP 6/ 270 December 1987

Die nachstehende Arbeit wurde im Rahmen des Vertrages zwischen dem Max-Planck-Institut für Plasmaphysik und der Europäischen Atomgemeinschaft über die Zusammenarbeit auf dem Gebiete der Plasmaphysik durchgeführt.

Alternative Constraints in the Entropy Principle for Tokamak Profiles Applied to Cylindrical Plasmas

Abstract

The recently proposed variational principle called the "entropy principle" /1/ is now applied with alternative constraints to cylindrical plasmas. These alternative constraints are that the pressure balance relation and Ohm's law with Spitzer conductivity and constant electric field should persist during the variations, replacing the constraint of fixed relations between the plasma pressure and density profiles used in /1/. This leads to a one-parameter family of slightly paramagnetic equilibria, the parameter being the internal plasma β. The safety factor ratio is found to be about 2. The corresponding plasmas are close to isentropic and their profiles agree reasonably well with Coppi's profile consistence formula for the temperature profiles /2/. A modification of Coppi's formula which greatly improves the agreement is given.

Introduction

In a recent paper /1/ we proposed a variational principle called the "entropy principle" which aims at yielding relations between the density profile $n(\vec{x})$ and pressure profile $p(\vec{x})$. We showed by comparison with experimental findings that tokamak plasmas in many cases have a tendency to relax to states in which these relations hold, being given by

$$p \;=\; n^{\gamma}\; e^{\alpha(1-1/n)} \tag{1}$$

with the normalization

$$p(\vec{x}_0) \;=\; n(\vec{x}_0) \;=\; 1 \qquad \vec{x}_0 \;:\; \textit{plasma center}\;. \tag{2}$$

Here γ is the adiabatic coefficient and $\alpha \geq 0$ is a constant which remains undetermined. In deriving these relations we assumed fast relaxation processes such that the entropy

$$S \;=\; \frac{1}{\gamma-1} \int\limits_{plasma} d^3x \left(n(\vec{x})\; ln \left(p(n(\vec{x}))\; n(\vec{x})^{-\gamma} \right) \;+\; (\gamma-1)\; s_0\; n(\vec{x}) \right), \tag{3a}$$

where s_0 is the entropy constant, no longer changes when the plasma performs arbitrary internal motions which are slow enough not to alter the relation $p(n)$ between the pressure profile $p(\vec{x})$ and the density profile $n(\vec{x})$.

In /1/ it was found that in the case of plane geometry relation (1) can also obtained in the following "alternative" way, which replaces the constraints of fixed $p(n)$ by "alternative" constraints:

The starting point is the entropy expression in the more general form

$$S \;=\; \frac{1}{\gamma-1} \int\limits_{plasma} d^3x \left(n(\vec{x})\; ln \left(p(\vec{x})\; n(\vec{x})^{-\gamma} \right) \;+\; (\gamma-1)\; s_0\; n(\vec{x}) \right), \tag{3b}$$

which does not contain any relation $p(n)$.
Let $B_t(x)$ be the "toroidal" field and $B_p(x)$ the "poloidal" field, and let $B_t >> B_p$.
The alternative constraints are then given by assuming that Spitzer's law or some similar law

$$j_t \;\sim\; T(x)^{1/\omega} \tag{4}$$

and the pressure balance relation

$$p(x) \;+\; \frac{1}{2}\left(B_t^2(x) \;+\; B_p^2(x) \right) \;=\; const \tag{5}$$

also hold during the slow variations. Then relation (1) follows from extremalizing the entropy (3b) by doing all the variations via $\delta B_p(x)$ with $\delta B_p = 0$ at the plasma surface. If, in addition, $B_t(x)$ is varied, α is found to be equal to zero.

This alternative way of extremalizing the entropy is pursued somewhat further in this paper. We treat a cylindrical plasma with circular cross-section; we do not require $B_t >> B_p$; we assume that Spitzer's law (11) for the current density parallel to $\vec{B}$ and the pressure balance relation (9) also hold during the slow variations of $B_t(r)$ and $B_p(r)$. All the varaions are subject to the constraints of fixed external magnetic field, fixed toroidal plasma current and zero pressure at the fixed plasma radius a. The resulting equations for $B_t(r)$ and $B_p(r)$ are solved for $\gamma = 5/3$ and different values of the plasma β. It turns out that the numerically obtained profiles roughly agree with relation (1) and with the relation

$$T(r) \;=\; exp\left(-\frac{2}{3}\,Q\,\frac{r^2}{n(r)^{1/5}}\right) \tag{6}$$

proposed by Coppi /2/ in the context of profile consistency. The main feature of our results is that the profiles for small plasma β correspond approximately to isentropic plasmas, i.e. $T = n^{2/3}$. In sec. 3 we present modifications of relations (1) and (6), which almost exactly describe our results.

2. Derivation of the equations for the magnetic field from the entropy principle

From Ampere's law

$$\vec{j} \;=\; curl\ \vec{B} \tag{7}$$

and the equilibrium relation

$$grad\ p \;=\; \vec{j} \times \vec{B} \tag{8}$$

one finds for axisymmetric cylindrical configurations the pressure balance equation

$$p(r) \;+\; \frac{1}{2}\Big(B_z^2(r) + B_\phi^2(r)\Big) + \int_0^r \frac{B_\phi^2(r')}{r'}dr' \;=\; 1 \;+\; \frac{1}{2}B_0^2\ , \tag{9}$$

where r, ϕ, z are cylindrical coordinates and $B_0 = B_z(r = 0)$ is the "toroidal" field at $r = 0$. The normalization is such that

$$p(r = 0) \;=\; n(r = 0) \;=\; 1. \tag{10}$$

Equation (9) is one of the four relations (9), (14), (24) ans (25) between $p(r)$, $T(r)$, $B_\phi(r)$ and $B_z(r)$. A second relation is obtained from Spitzer's law for the current density parallel to $\vec{B}$:

$$E_{||} \;=\; \eta_{||}\, j_{||} \;\sim\; T^{-3/2}\, j_{||}\ , \tag{11}$$

where $E_{||}$ is the component of the r-independent external toroidal electric field parallel to $\vec{B}$:

$$E_{||} \;=\; \vec{E}\,\frac{\vec{B}}{B} \;=\; E\,\frac{B_z}{B}\;. \tag{12}$$

Similarly, we have

$$j_{||} \;=\; j_z\,\frac{B_z}{B} \;+\; j_\phi\,\frac{B_\phi}{B}\;. \tag{13}$$

Such a normalization can be used so that eqs. (11-13) can now be written as

$$T^{3/2} \;=\; j_z \;+\; j_\phi\,\frac{B_\phi}{B_z} \;=\; \frac{1}{r}\,\frac{\partial}{\partial r}(rB_\phi) \;-\; \frac{B_\phi}{B_z}\,\frac{\partial B_z}{\partial r}\;. \tag{14}$$

This normalization together with

$$p(r=0) \;=\; n(r=0) \;=\; 1$$

means

$$T(r=0) \;=\; j_z(r=0) \;=\; 1. \tag{15}$$

Equations (9) and (14) allow us to express δp and δT, and hence our whole variational expression, in terms of δB_z and δB_ϕ. With $\gamma = 5/3$ and with λ being the Lagrange parameter for the constraint of fixed total number of particles, the variational principle can be written as

$$\delta \int_0^a L\,r''\,dr'' \;=\; \int_0^a dr''\,r''\left(\frac{\partial L}{\partial p}\,\delta p \;+\; \frac{\partial L}{\partial T}\,\delta T\right) \;=\; 0, \tag{16}$$

with

$$L \;=\; \frac{p}{T}\left(\frac{5}{3}\,ln\,T \;-\; \frac{2}{3}\,ln\,p \;+\; \lambda\right) \tag{17}$$

and a = plasma radius. Equation (9) yields

$$\delta p \;=\; B_0\,\delta B_0 - B_\phi\,\delta B_\phi \;-\; B_z\,\delta B_z \;-\; 2\int_0^r \frac{B_\phi(r')\;\delta B_\phi(r')}{r'}\,dr'\;. \tag{18}$$

The constraints of fixed external magnetic field, fixed toroidal plasma current and zero pressure at the fixed plasma radius a mean

$$\delta B_z(a) \;=\; \delta B_\phi(a) \;=\; \delta p(a) \;=\; 0\;,$$

which with eq. (18) for $r = a$ gives

$$B_0\,\delta B_0 \;=\; 2\int_0^a \frac{B_\phi(r')\delta B_\phi(r')}{r'}\,dr' \tag{19}$$

and therefore

$$\delta p \;=\; -\,B_\phi\;\delta B_\phi - \;B_z\;\delta B_z \;+\; 2\int\limits_r^a \frac{B_\phi(r')\delta B_\phi(r')}{r'}\;dr'\;. \tag{20}$$

Equation (14) yields

$$\delta T \;=\; \frac{2}{3\sqrt{T}}\left[\frac{1}{r}\frac{d}{dr}(r\;\delta B_\phi) \;-\; \frac{\delta B_\phi}{B_z}\;\frac{dB_z}{dr} \;-\; B_\phi\;\frac{d}{dr}\left(\frac{\delta B_z}{B_z}\right)\right]. \tag{21}$$

We can now evaluate eq. (16) with

$$\delta B_\phi(\hat{r}) \;=\; \delta B_\phi^0\;\delta(\hat{r}-r) \quad\;,\;\; \delta B_z(\hat{r}) \;=\; \delta B_z^0\;\delta(\hat{r}-r)\;, \tag{22}$$

where δB_ϕ^0 , δB_z^0 are arbitrary constants; $\hat{r}$ can be r' or r'' . It follows that

$$\begin{aligned}\delta\int\limits_0^a L\;r''\;dr'' \;=\; 2\int\limits_0^r dr''\;r''\;\frac{\partial L}{\partial p}\bigg|_{r''}\;\frac{B_\phi(r)}{r}\;\delta B_\phi^0 \;+\\ -\;r\left(B_\phi\;\delta B_\phi^0 + B_z\;\delta B_z^0\right)\frac{\partial L}{\partial p} \;+\\ -\;\frac{2}{3}\;\frac{r}{\sqrt{T}}\;\frac{\partial L}{\partial T}\;\frac{1}{B_z}\;\frac{dB_z}{dr}\;\delta B_\phi^0 \;+\\ -\;\frac{2}{3}\;r\;\frac{d}{dr}\left(\frac{1}{\sqrt{T}}\;\frac{\partial L}{\partial T}\right)\delta B_\phi^0 \;+\\ +\;\frac{2}{3}\;\frac{d}{dr}\left(r\;B_\phi\;\frac{1}{\sqrt{T}}\;\frac{\partial L}{\partial T}\right)\;\frac{1}{B_z}\;\delta B_z^0\;.\end{aligned} \tag{23}$$

This expression must be zero for any choice of δB_ϕ^0 and δB_z^0 and therefore the following equations for $B_\phi(r)$ and $B_z(r)$ must hold:

$$\frac{\partial L}{\partial p}\;B_\phi \;-\; \frac{2}{r^2}\;B_\phi\int\limits_0^r dr''r''\frac{\partial L}{\partial p}\bigg|_{r''} \;+\; \frac{2}{3\sqrt{T}}\;\frac{\partial L}{\partial T}\;\frac{1}{B_z}\;\frac{dB_z}{dr} \;+\; \frac{d}{dr}\left(\frac{2}{3\sqrt{T}}\;\frac{\partial L}{\partial T}\right) \;=\; 0\;, \tag{24}$$

$$\frac{\partial L}{\partial p}B_z \;-\; \frac{1}{r}\;\frac{1}{B_z}\;\frac{d}{dr}\left(r\;B_\phi\;\frac{2}{3\sqrt{T}}\frac{\partial L}{\partial T}\right) \;=\; 0\;. \tag{25}$$

3. Numerical results and comparison with relations (1) and (6)

Equations (24) and (25) have to be solved with the boundary conditions at $r = 0$ (see eqs.(9), (10), (15)):

$$B_z = B_0 \; ; \quad \frac{dB_z}{dr} = 0 \; , \tag{26}$$

$$B_\phi = 0. \; ; \quad \frac{dB_\phi}{dr} = \frac{1}{2} \; . \tag{27}$$

There are therefore two constants, B_0 and λ, in the problem. However, λ is determined by B_0 with the relation

$$\lambda = \frac{\frac{5}{3} + B_0^2}{1 + \frac{3}{2} B_0^2} \; , \tag{28}$$

which follows from eq. (25) at $r = 0$ and the boundary conditions (10), (15), (26), (27). On the other hand, B_0 is related to the internal plasma β defined by

$$\beta_i = \frac{p(r=0)}{B^2(r=0)/2} = \frac{2}{B_0^2} \; , \tag{29}$$

which is therefore the only free parameter.

Equations (9), (14), (24) and (25) were solved numerically for the following set of values:

$$B_0 = 2 \; ; \; 3 \; ; \; 5 \; ; \; 8 \; ,$$

which is equivalent to

$$\beta_i = 0.5 \; ; \; 0.22 \; ; \; 0.08 \; ; \; 0.031 \; .$$

Figures 1 show the toroidal field B_z (solid) and the poloidal field B_ϕ (dashed) as functions of r together with the approximations B_{za} (crossed) and $B_{\phi a}$ (rhombuses) given by

$$B_z \approx B_{za} = B_0 - \frac{Z_2 \, r^2}{1 + 0.035 \, r^2 \, (1 + 0.08 r^2)} \; , \tag{30a}$$

with

$$Z_2 = 0.1 \sqrt{\frac{\beta_i}{1 + \beta_i}} \; , \tag{30b}$$

and

$$B_\phi \approx B_{\phi a} = \frac{r}{2} \left(1 - \frac{\phi_2 \, r^2}{1 + (0.063 + 0.14 \, \beta_i) \, r^2} \right) \; , \tag{30c}$$

with

$$\phi_2 = \frac{0.028 + 0.1 \, \beta_i}{1 + 0.5 \, \beta_i} \; . \tag{30d}$$

The approximations (30) hold for $\beta_i \leq 0.22$ and $r < a$. The safety factor ratio

$$\frac{q_a}{q_0} = \frac{a}{2B_0} \frac{B_z(a)}{B_\phi(a)} \tag{31a}$$

is related to β_i by

$$\frac{q_a}{q_0} \approx 1.8 + \beta_i \tag{31b}$$

for $\beta_i \leq 0.5$.

Figures 2 show the corresponding density n (solid) and temperature profiles T (dashed) and, in addition, the temperature profiles (crossed)

$$T_E = n^{2/3} e^{\alpha(1-1/n)} , \tag{32a}$$

which follow from the numerically obtained density n and relation (1), with

$$\alpha \approx \frac{0.2\,\beta_i}{1 + 2.5\beta_i^2} , \quad \beta_i \leq 0.5 , \tag{32b}$$

chosen such as to get optimum agreement between T and T_E. The agreement between T and T_E is excellent for small β_i owing to the smallness of α. With increasing β_i disagreement caused by α/n in the exponent of eq. (32a) arises in the plasma edge region and becomes serious there for, say, $\beta > 0.2$. In the interior plasma region the agreement remains fair. According to eq. (32b), all α values occurring in this model are small in relation to 1 and describe almost isentropic plasmas, which are often realized in large tokamaks with ohmic heating.

Figures 3 show the numerically obtained density $n(r)$ (solid) and temperature profiles $T(r)$ (dashed) together with the temperature profiles $T_C(r)$ (crossed), obtained from Coppi's formula

$$T_C(r) = exp\left(-\frac{2}{3}\, Q\, \frac{r^2}{n(r)^{1/5}}\right) , \tag{6}$$

and the numerically obtained densities $n(r)$, with

$$Q \approx 0.066$$

chosen such as to get optimal agreement between T and T_C. There is fair agreement, except for small β_i in the plasma edge region.

It is found from the numerical results that a temperature-density relation similar to (32a), namely

$$T \approx T_P = n^{2/3} e^{\hat{\alpha} n - \hat{\alpha}} , \tag{33a}$$

with

$$\hat{\alpha} = \frac{0.45\beta_i}{1+\beta_i} , \tag{33b}$$

is satisfied excellently for $\beta_i \leq 0.5$ and fairly well (a few per cent) for up to $\beta_i = 2$. Relation (34a) follows from (32a), if α is replaced by $\alpha = \hat{\alpha} n$.

Furthermore, the density profile can be approximated by $n_P(r)$, which we write in the inverse form

$$r = \sqrt{-n_P^{\epsilon} \frac{ln\ n_P}{Q}} , \tag{34a}$$

with

$$Q = \frac{0.0564 + 0.056\ \beta_i}{\sqrt{1 + 0.8\ \beta_i^2}} \tag{34b}$$

and

$$\epsilon = 0.39 - 0.065\ \beta_i - 0.8\ \sqrt{\beta_i}\ n . \tag{34c}$$

Relation (34) is excellently satisfied for $\beta_i \leq 0.22$ and, furthermore, for $\beta_i = 0.5$ and $n \geq 0.3$; serious disagreement arises for $\beta_i \geq 0.5$ in the plasma edge region. Relation (34) can be interpreted as a combination profile which is obtained by combining relation (33a) with Coppi's relation (6), by having ϵ instead of $1/5$ in the exponent, and by negelcting $\hat{\alpha}$. From eqs.(33) and (34) we find a modified Coppi relation

$$T_Q = exp\left(-\frac{2}{3}\frac{Q\ r^2}{n^{\epsilon}} + \hat{\alpha}\ (n - 1)\right) , \tag{35}$$

which holds instead of eq.(6) in our plasma model. The difference between the temperatures T and T_Q is relevant only for $\beta_i = 0.5$ and, say, $T \leq 0.2$ and causes disagreement between the numerical density profile and eq.(34).

Figures 4 show once more the temperature profiles $T(r)$ (dashed) and density profiles $n(r)$ (solid) together with the approximations T_P (crossed) for the temperature and n_P (rhombuses) for the density.

4. Conclusions

In this paper we have evaluated the entropy principle for a cylindrical plasma in a way different to that in /1/. The difference between this paper and /1/ is in the constraints:
- in /1/ we assumed $p(n)$ to be unaltered during the variations;
- in this paper $\delta p(r)$ and $\delta T(r)$ are obtained by assuming that the equilibrium pressure balance relation (9) and Ohm's law (11) with Spitzer conductivity also hold during the variations.

These variations are expressed in terms of $\delta B_\phi(r)$ and $\delta B_z(r)$; see eqs.(20) and (21). There was then only one free parameter left to characterize the different solutions of the problem: the internal plasma β (named β_i ; see eq.(29)).

The difference between the results of this paper and those of /1/ might be characterized by the exponent in the $T(n)$ relation:
- in /1/ this exponent is $\alpha(1 - 1/n)$; see eq.(32),
- in this paper we have $\hat{\alpha}(n - 1)$; see eq.(33).

For all β_i the plasmas turned out to be paramagnetic. The safety factor ratio q_a/q_0 is about 2 and is related to β_i according to eq.(31b). A comparison with the entropy principle used in /1/, which leads to relation (1), shows fair agreement for β_i up to 0.2 and excellent agreement for, say, $\beta_i < 0.1$, except for the plasma edge region, where the difference between eq.(32) and (33) becomes serious. The values of α in eq.(1) are about $0.2\ \beta_i$ (see eq.(32b)) and are always small in relation to one. The model plasmas obtained by our alternative entropy principle are therefore close to isentropic, a situation which seems to be realized the better the larger the machines are. There is also more or less reasonable agreement with Coppi's relation (6).

Equations (33) and (34) represent good approximations for the $n(r)$ and $T(r)$ profiles resulting from our alternative entropy principle - except for sufficiently large β_i in the plasma edge region, as discussed in connection with figs.(4). A comparison of the experimental profiles presented in /1/ shows that eqs.(1) and (6) can be used to fit the experimental data just as well as eqs.(33) and (34) - except in cases like pellet injection, where neither eqs.(1), (6) nor eqs.(33),(34) can be used. The reason is that the difference between eqs.(1),(6) and eqs.(33),(34) is mainly in the edge region, where no sufficiently exact data are available.

Whereas the alternative form of our entropy principle allows only plasma profiles close to isentropic, the original form with fixed $p(n)$ leading to relation (1) also allows large deviations from isentropic. This means that the "old" constraints with $p(n)$ allow lower entropies of the plasmas than the new ones do. The entropy resulting from eqs.(3) and (1) is

$$S \;=\; s_0 N \;-\; \frac{\alpha}{\gamma - 1}\left(n_0 V \;-\; N\right), \qquad (36)$$

where N is the total number of particles, n_0 the central plasma density and V the plasma volume. Since $n_0 V > N$, large α values mean small entropies.

Two time scales might therefore exist, as already mentioned in /1/:
- a faster one describing relaxation towards states where α is not necessarily small, which might have to do with the constraint of fixed $p(n)$;
- a slower one describing relaxation towards states with $\alpha << 1$, which might have to do

with the equilibrium constraints used in this paper.

References

/1/ D.Pfirsch and F.Pohl, Plasma Physics and Controlled Fusion, **29**, 697, (1987)
/2/ B.Coppi, Comments Plasma Phys. Contr. Fusion **5**, 261, (1980)

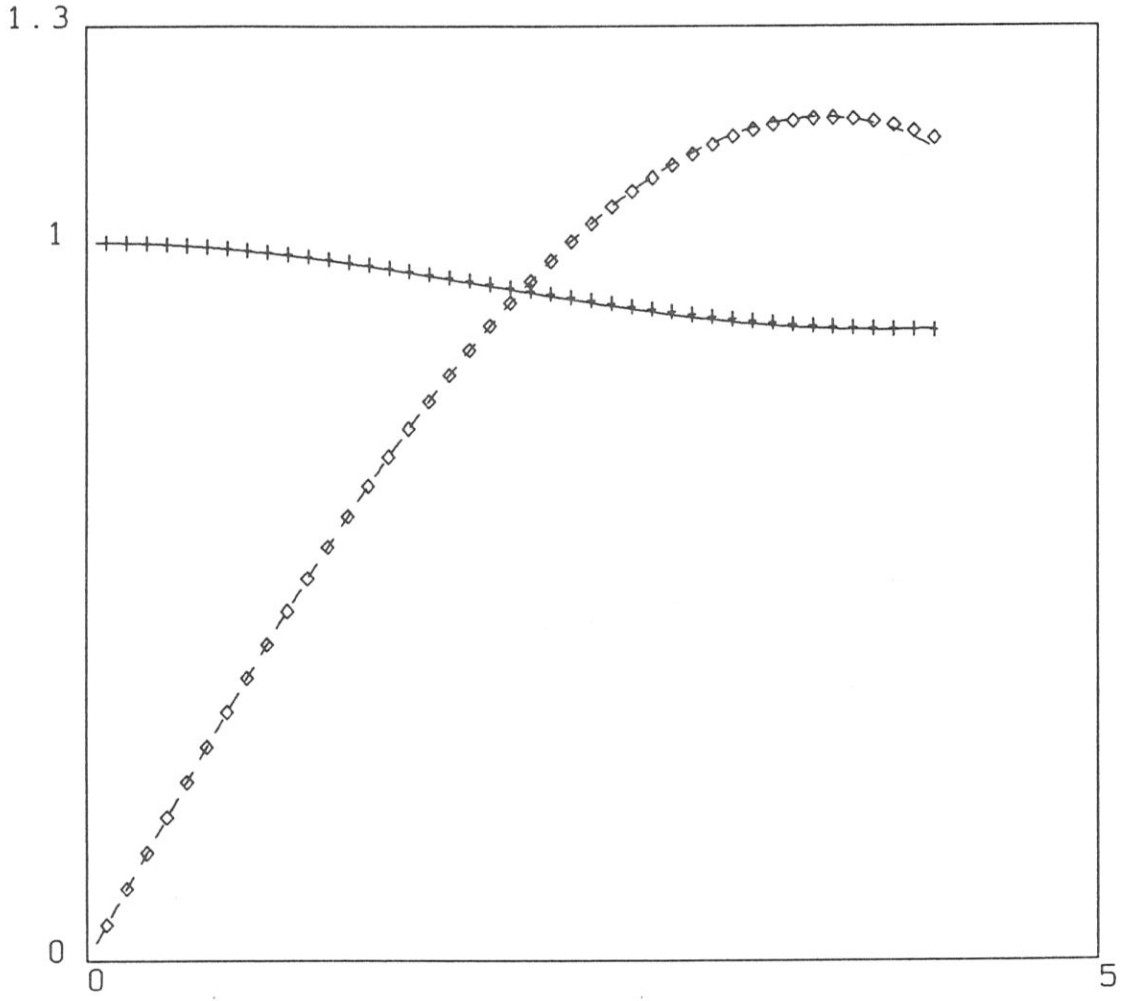

Fig 1a
Toroidal field B_z (solid: $B_z + 1 - B_0$)
and poloidal field B_ϕ (dashed) vs. r
for $\beta_i = 0.031$, $B_0 = 8.$,
together with the approximations (30)
B_{za} (crossed) and $B_{\phi a}$ (rhombuses)

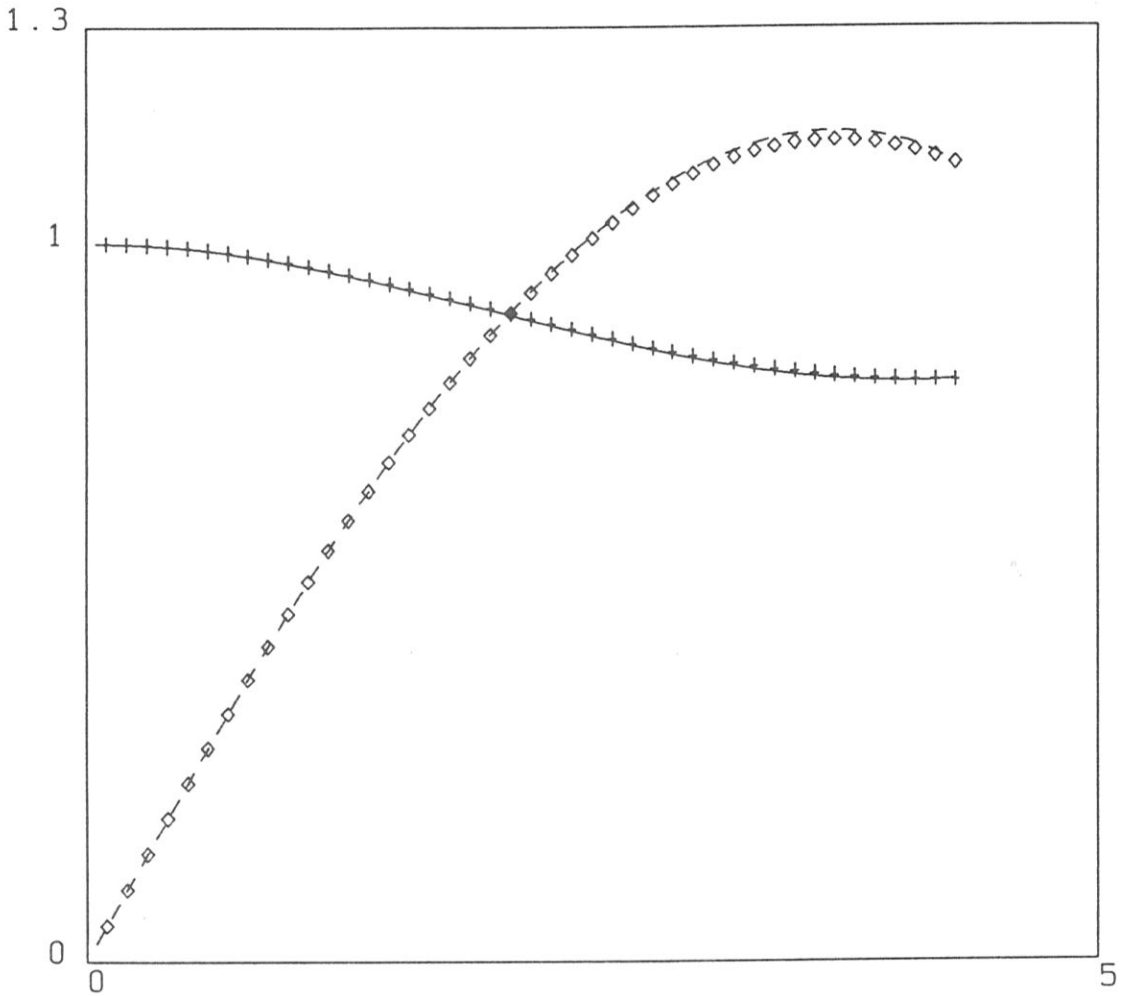

Fig 1b
Toroidal field B_z (solid: $B_z + 1 - B_0$)
and poloidal field B_ϕ (dashed) vs. r
for $\beta_i = 0.08$, $B_0 = 5.$,
together with the approximations (30)
B_{za} (crossed) and $B_{\phi a}$ (rhombuses)

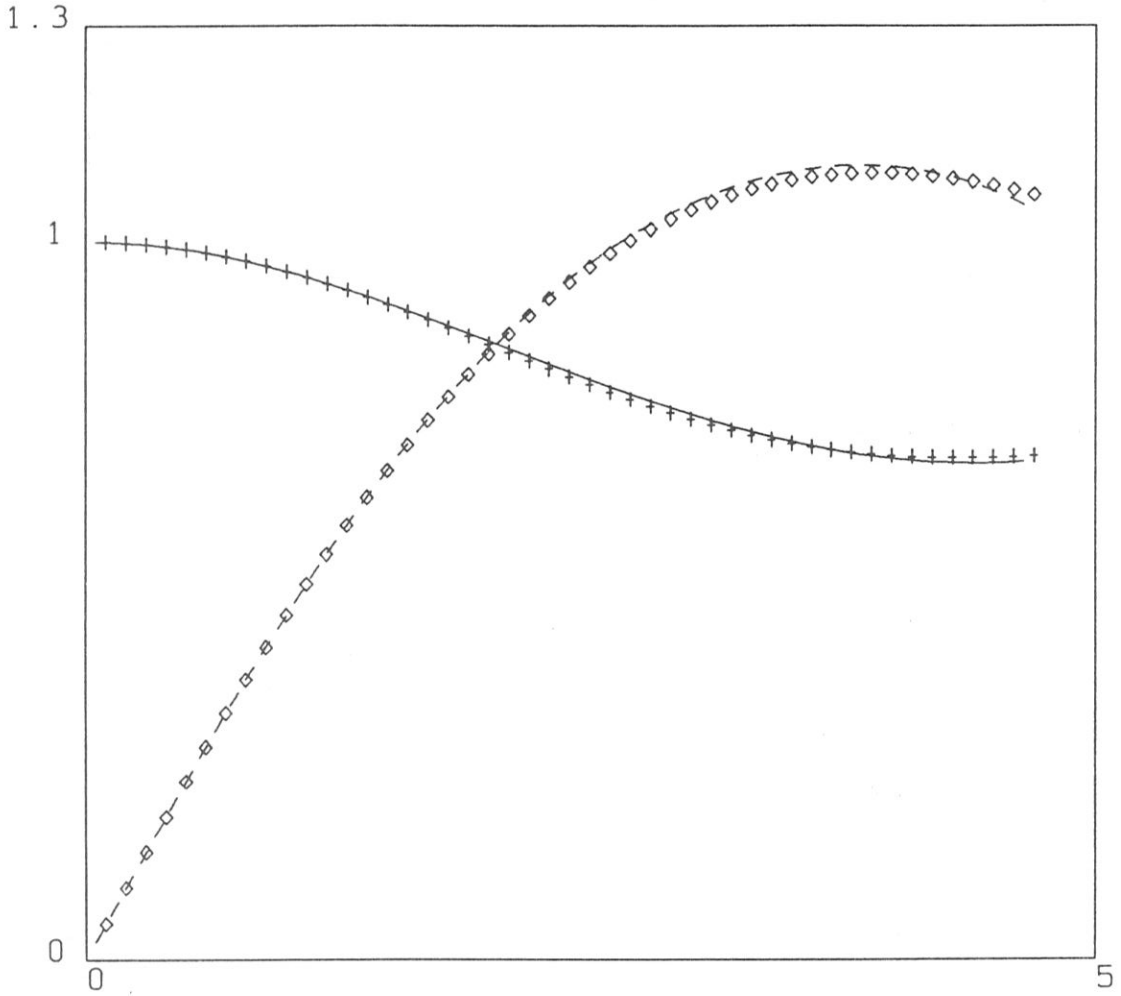

Fig 1c
Toroidal field B_z (solid: $B_z + 1 - B_0$)
and poloidal field B_ϕ (dashed) vs. r
for $\beta_i = 0.222$, $B_0 = 3.$,
together with the approximations (30)
B_{za} (crossed) and $B_{\phi a}$ (rhombuses)

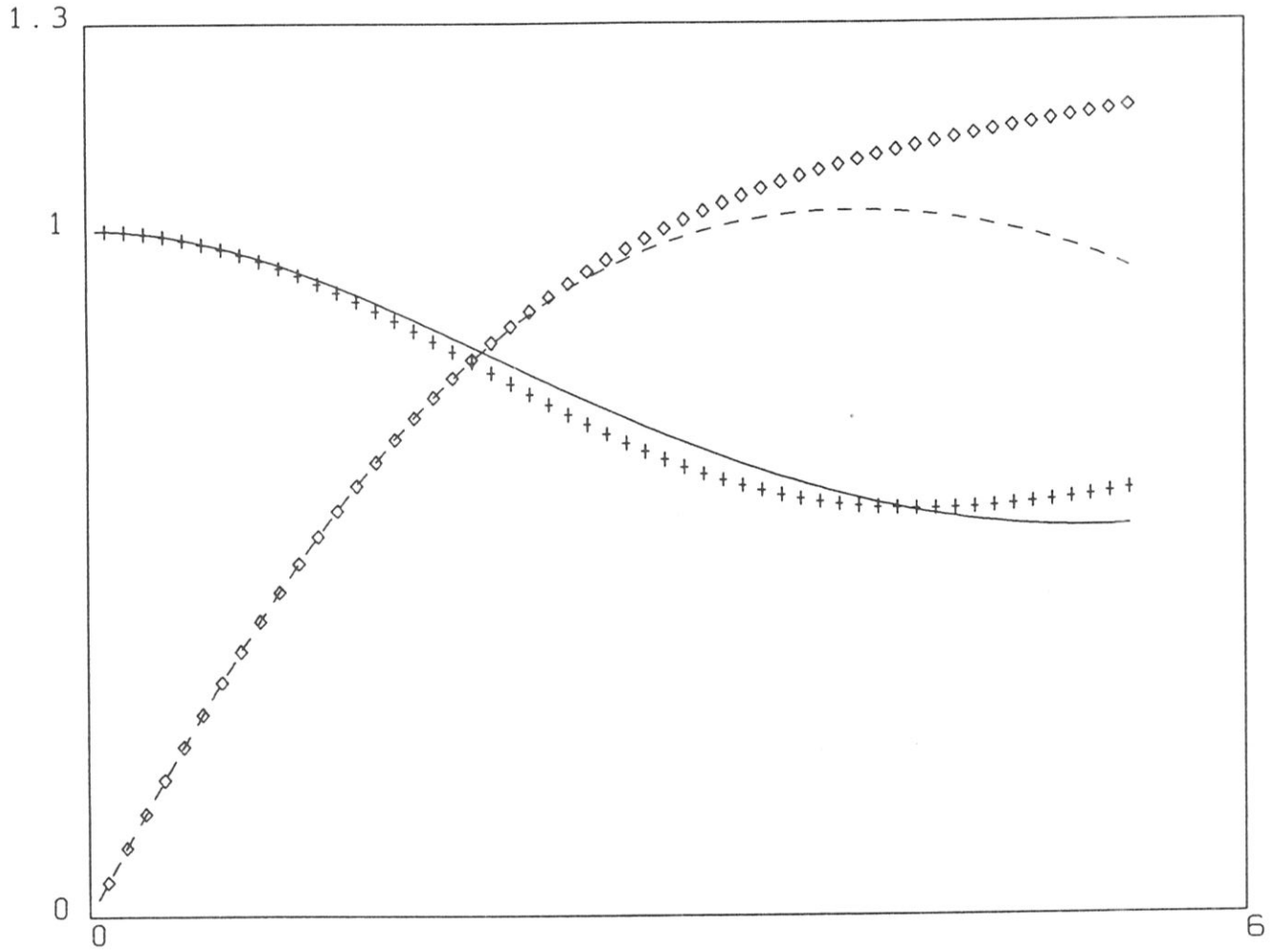

Fig 1d
Toroidal field B_z (solid: $B_z + 1 - B_0$)
and poloidal field B_ϕ (dashed) vs. r
for $\beta_i = 0.5$, $B_0 = 2.$,
together with the approximations (30)
B_{za} (crossed) and $B_{\phi a}$ (rhombuses)

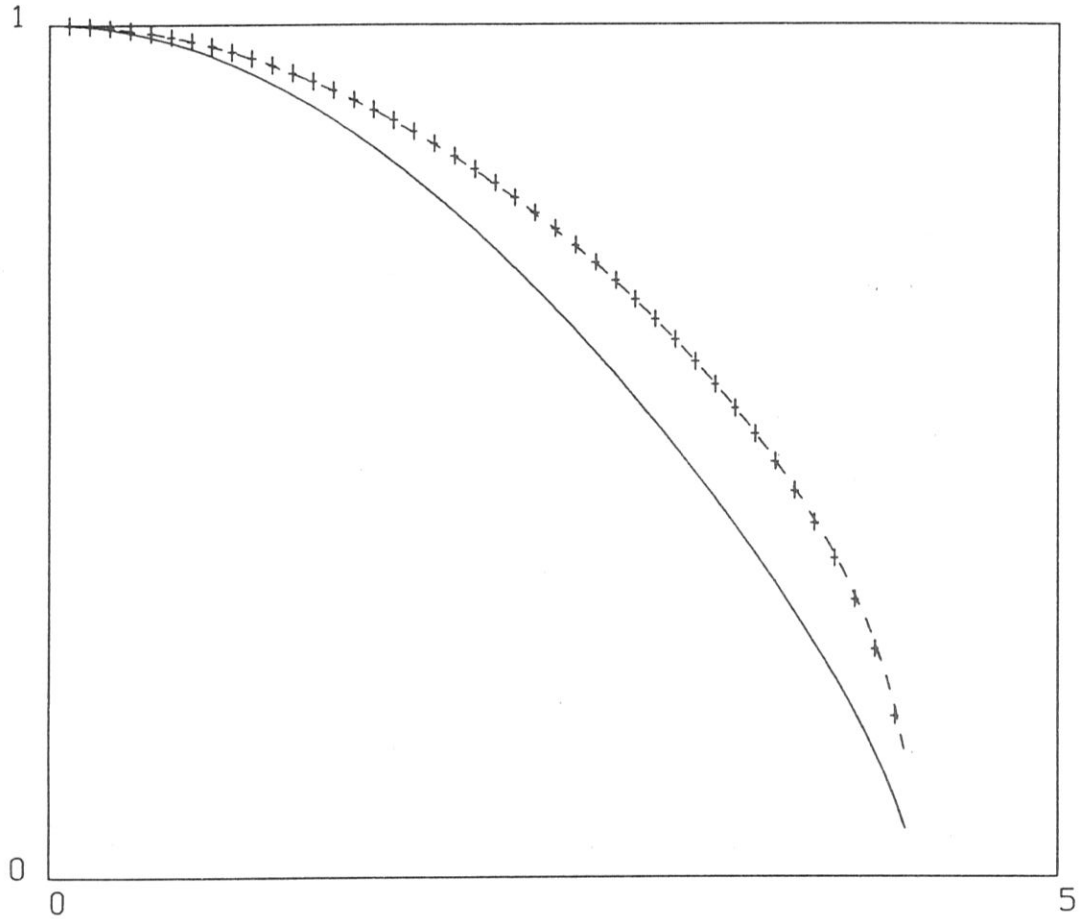

Fig. 2a
Density and temperature vs. r
for $\beta_i = 0.031$, $\alpha = 0.007$

Solid : density , numerical
Dashed: temperature, numerical
Crossed: temperature acc. to eq.(32)
$T_E = n^{\gamma-1}\, e^{\alpha(1-1/n)}$

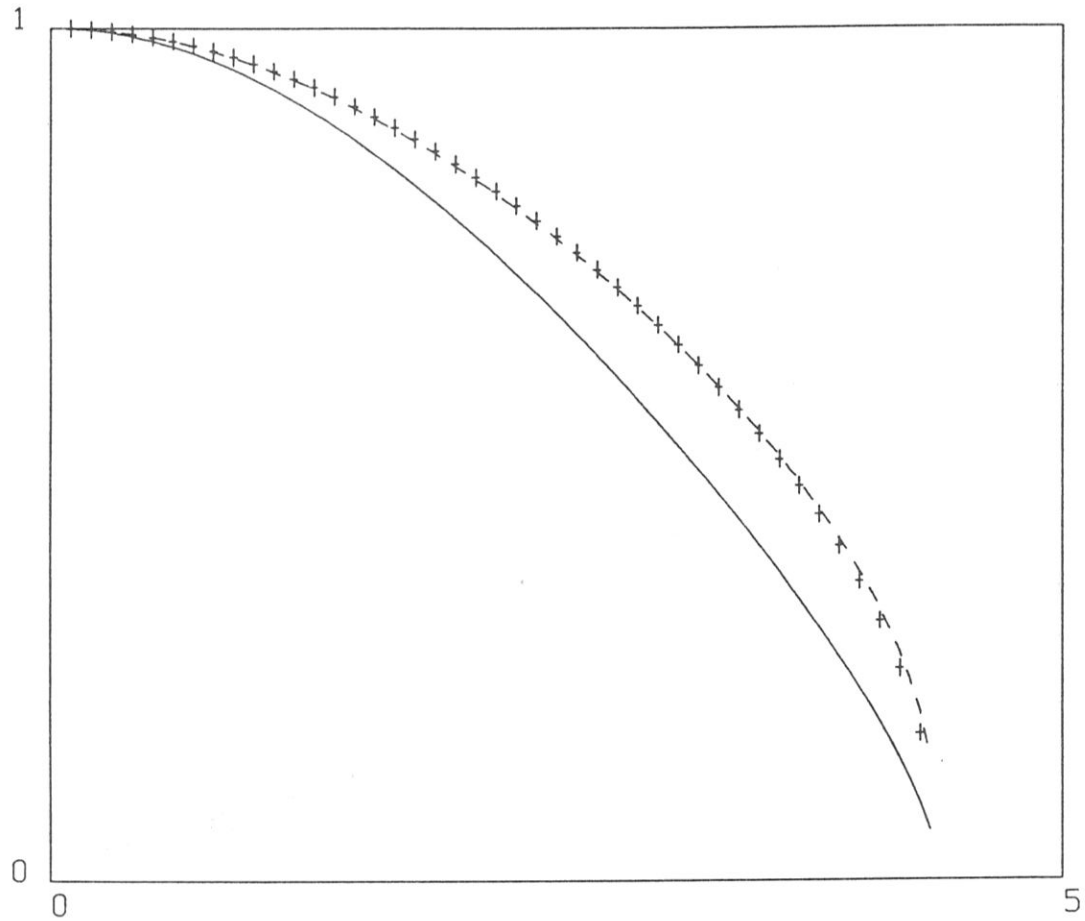

Fig. 2b
Density and temperature vs. r
for $\beta_i = 0.08$, $\alpha = 0.016$

Solid : density , numerical
Dashed: temperature, numerical
Crossed: temperature acc. to eq.(32)
$T_E = n^{\gamma-1}\, e^{\alpha(1-1/n)}$

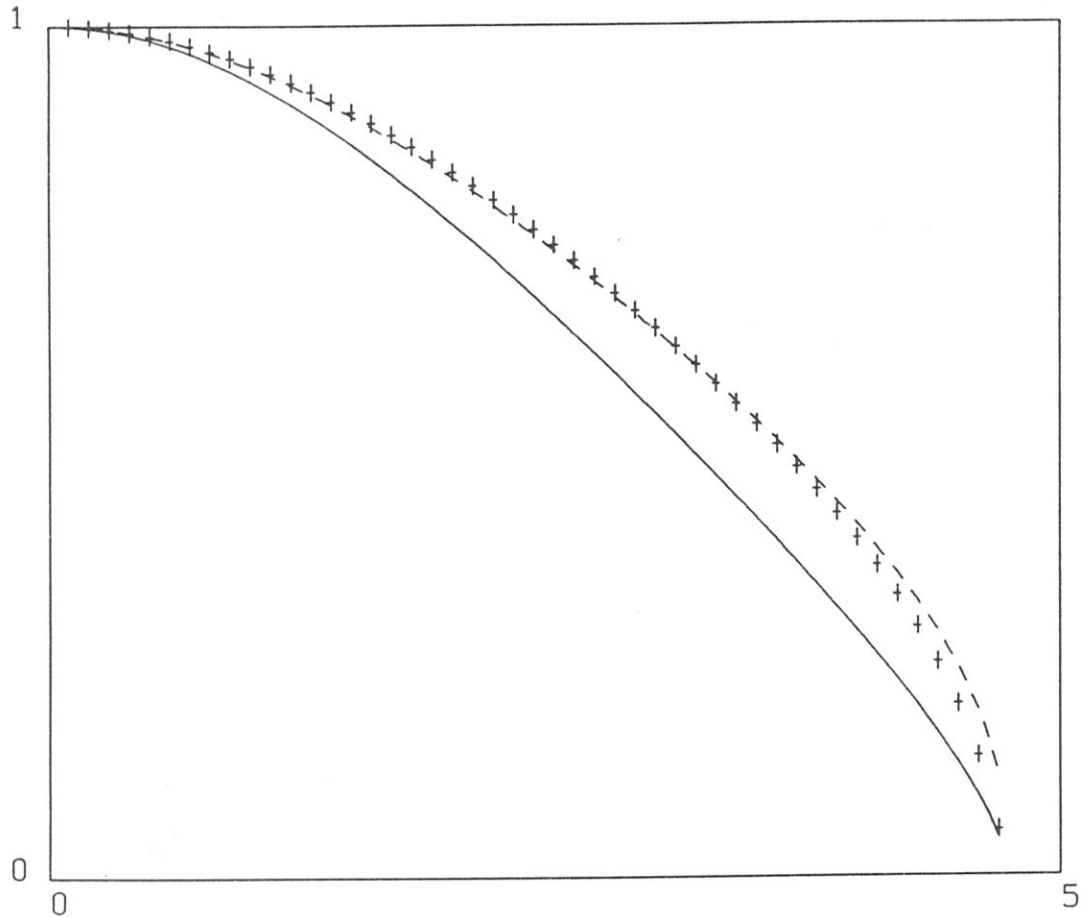

Fig. 2c
Density and temperature vs. r
for $\beta_i = 0.222$, $\alpha = 0.038$

Solid : density , numerical
Dashed: temperature, numerical
Crossed: temperature acc. to eq.(32)
$T_E = n^{\gamma-1}\, e^{\alpha(1-1/n)}$

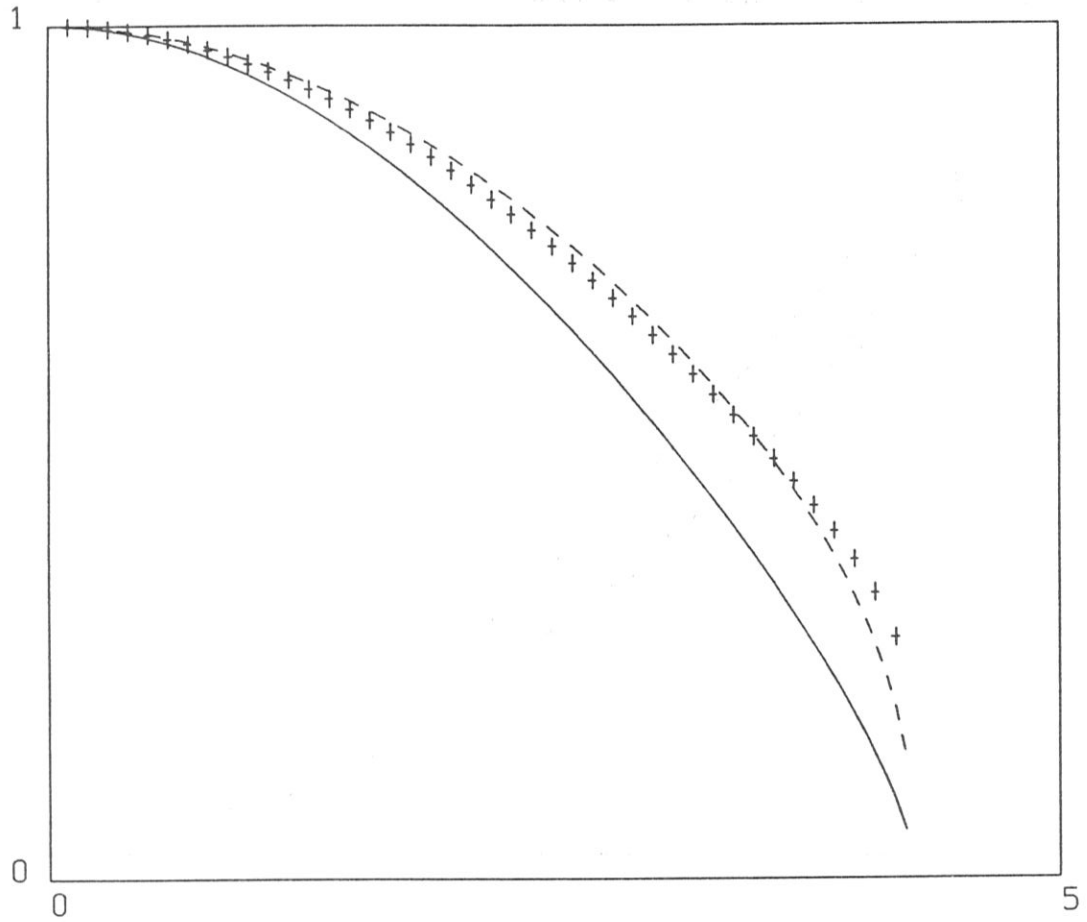

Fig. 3a
Density and temperature vs. r
for $\beta_i = 0.031$
Solid : density , numerical
Dashed: temperature, numerical
Crossed: Coppi temperature, acc. to eq.(6)
$T_C(r) = exp\left(-\frac{2}{3}\, Q\, \frac{r^2}{n(r)^{1/5}}\right)$,

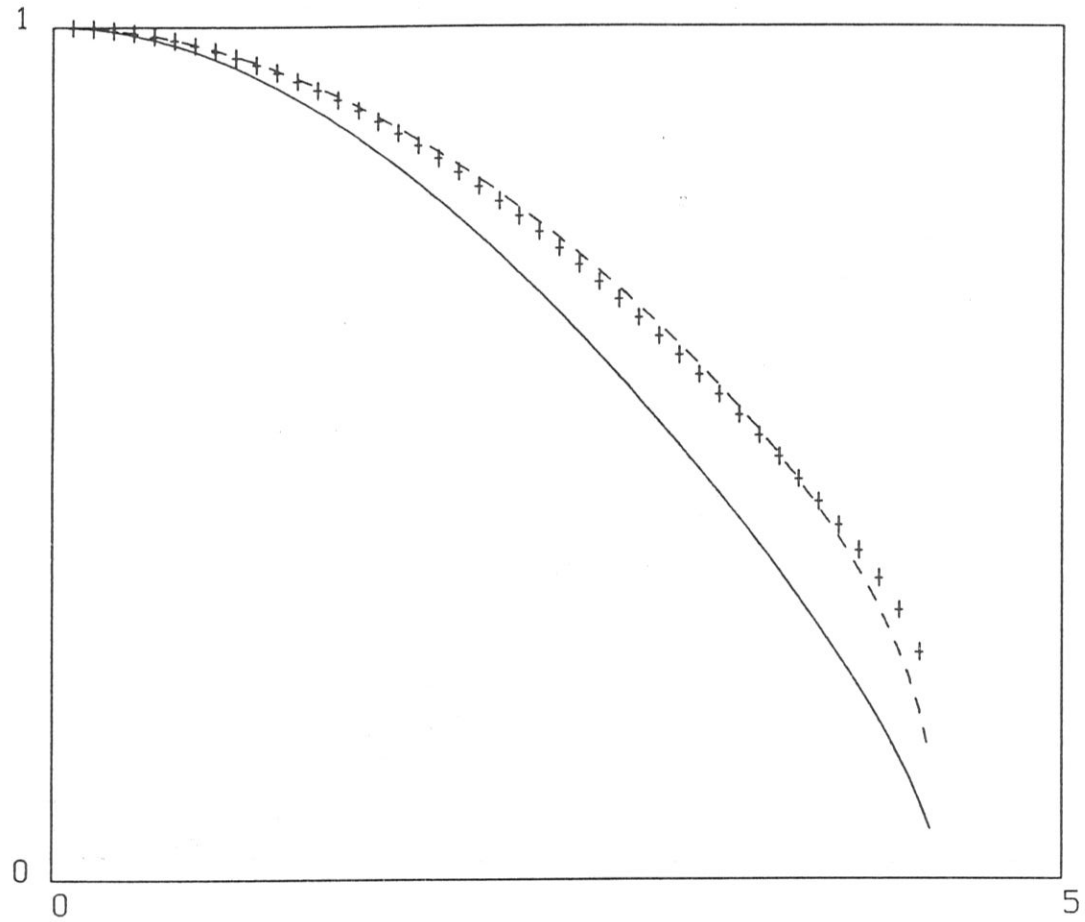

Fig. 3b
Density and temperature vs. r
for $\beta_i = 0.08$
Solid : density , numerical
Dashed: temperature, numerical
Crossed: Coppi temperature, acc. to eq.(6)
$T_C(r) = exp\left(-\frac{2}{3} Q \frac{r^2}{n(r)^{1/5}}\right)$,

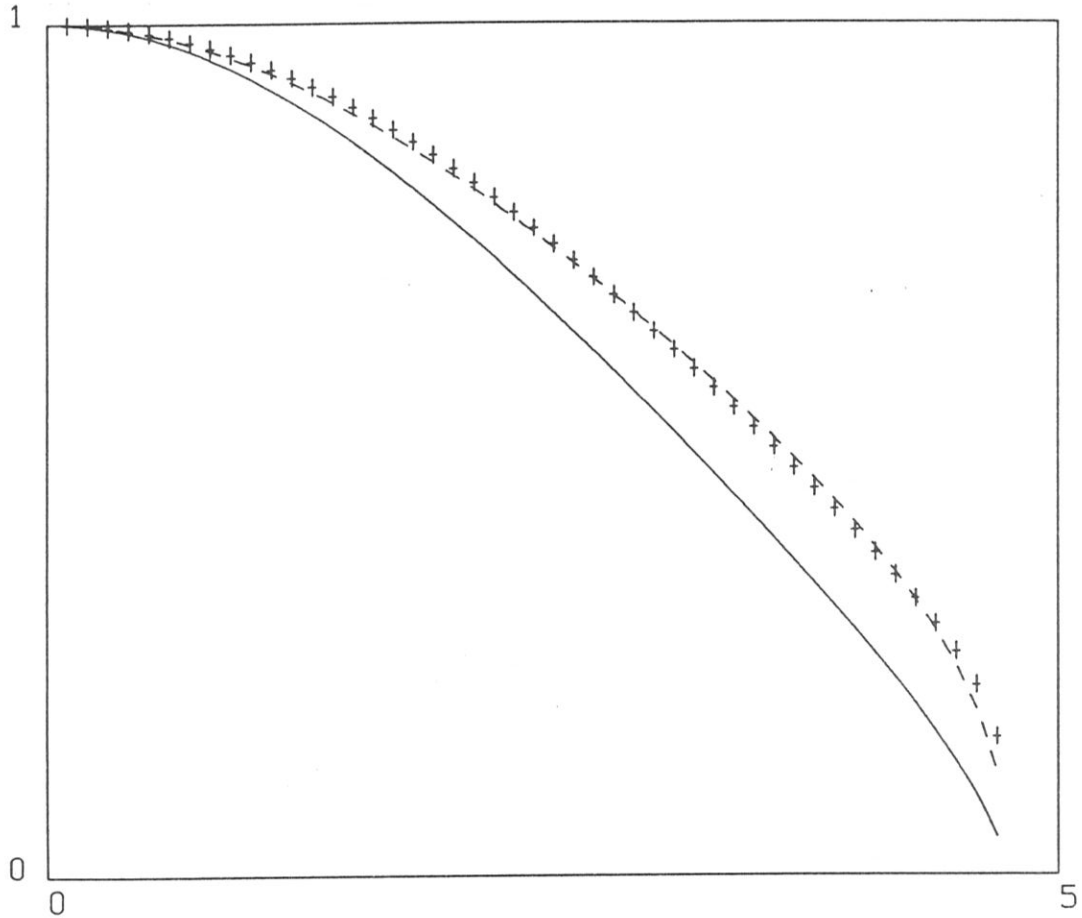

Fig. 3c
Density and temperature vs. r
for $\beta_i = 0.222$
Solid : density , numerical
Dashed: temperature, numerical
Crossed: Coppi temperature, acc. to eq.(6)
$T_C(r) = exp\left(-\frac{2}{3}\, Q\, \frac{r^2}{n(r)^{1/5}}\right)$,

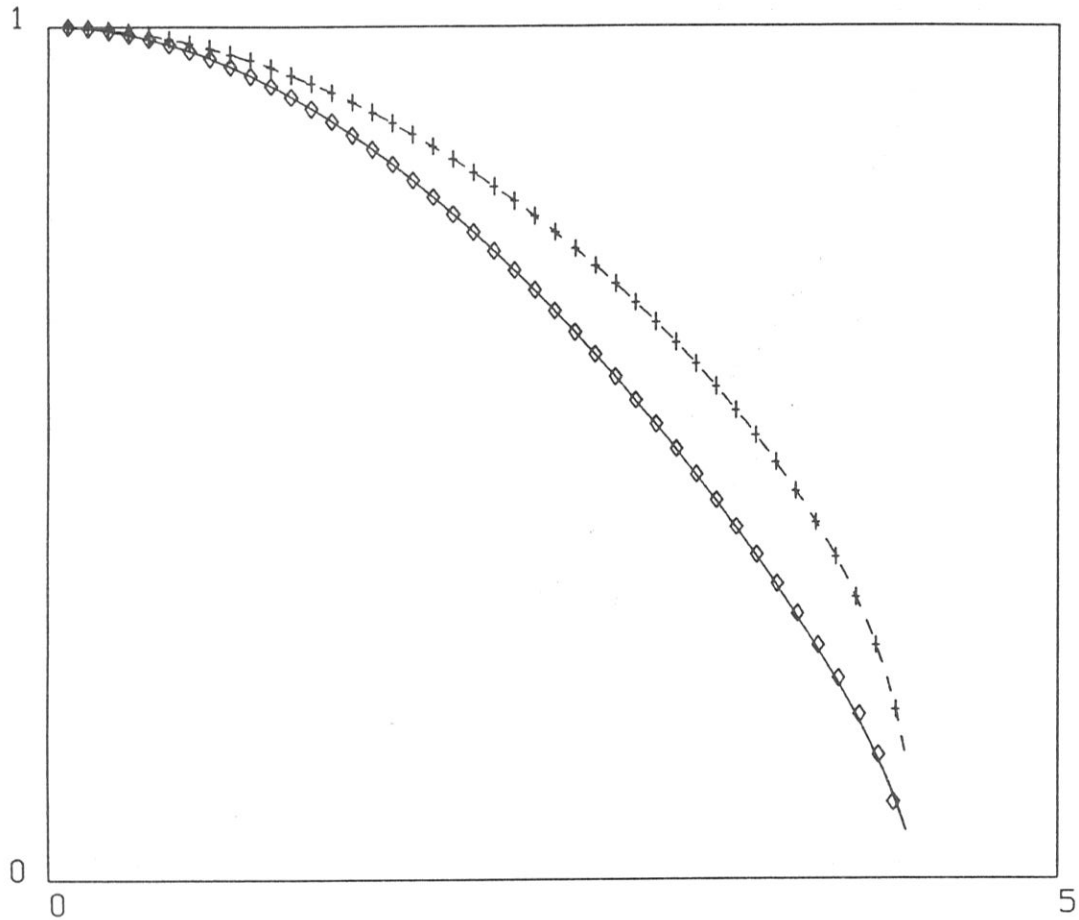

Fig. 4a
Density and temperature vs. r
for $\beta_i = 0.031$
Solid : density , numerical
Dashed: temperature, numerical
Crossed: temperature, acc. to eq.(33)
$T_P = n^{2/3}\, e^{\hat{\alpha}n - \hat{\alpha}}$
Rhombuses: density, acc. to eq.(34)
$r = \sqrt{-n_P^{\epsilon}\, \frac{ln\ n_P}{Q}}$

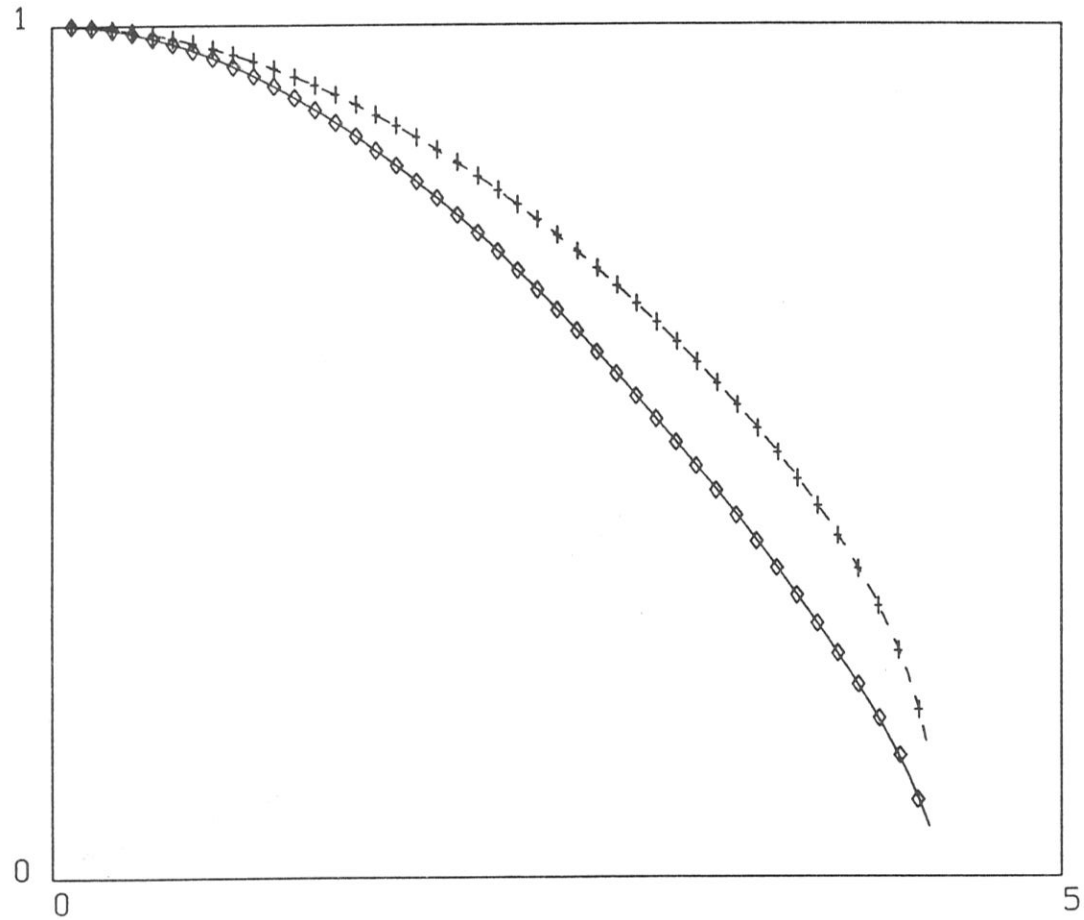

Fig. 4b
Density and temperature vs. r
for $\beta_i = 0.08$
Solid : density , numerical
Dashed: temperature, numerical
Crossed: temperature, acc. to eq.(33)
$T_P = n^{2/3}\, e^{\hat{\alpha} n - \hat{\alpha}}$
Rhombuses: density, acc. to eq.(34)
$r = \sqrt{-n_P^{\epsilon}\, \frac{ln\ n_P}{Q}}$

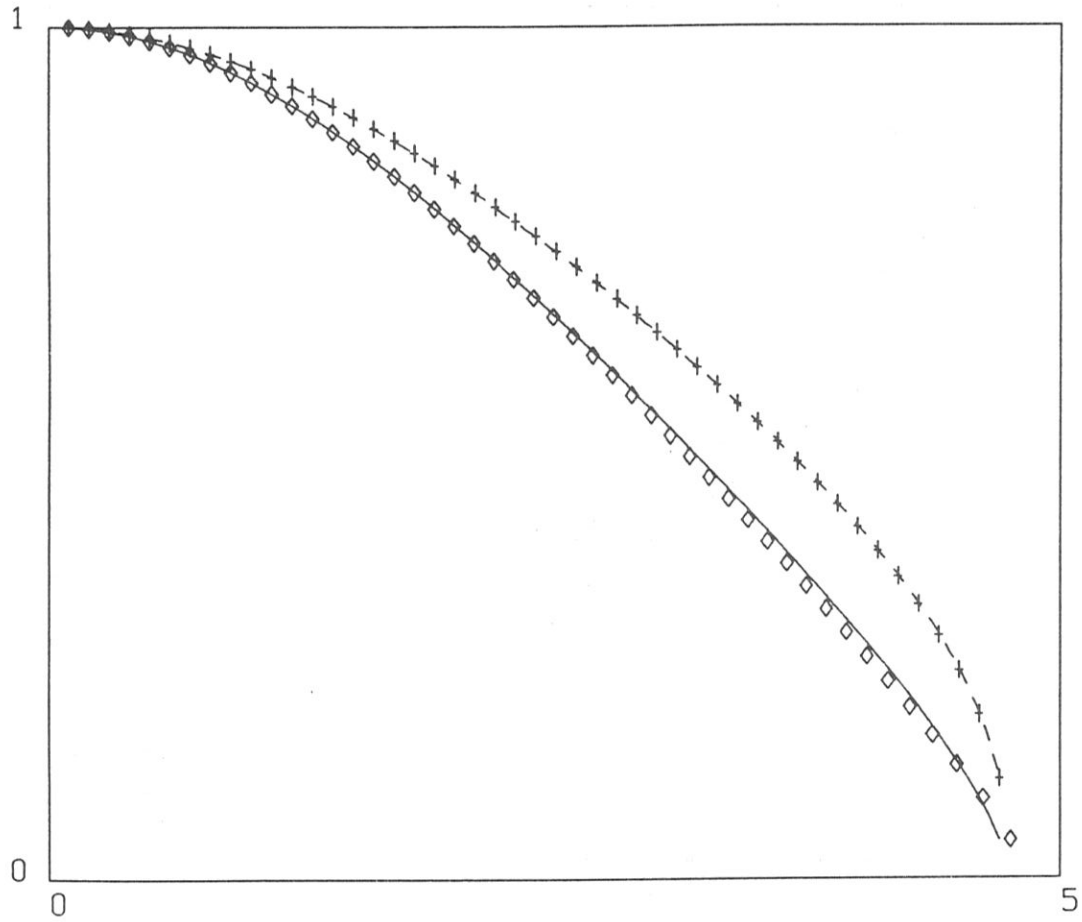

Fig. 4c
Density and temperature vs. r
for $\beta_i = 0.222$
Solid : density , numerical
Dashed: temperature, numerical
Crossed: temperature, acc. to eq.(33)
$T_P = n^{2/3}\, e^{\hat{\alpha} n - \hat{\alpha}}$
Rhombuses: density, acc. to eq.(34)
$r = \sqrt{-n_P^{\epsilon}\, \frac{ln\ n_P}{Q}}$

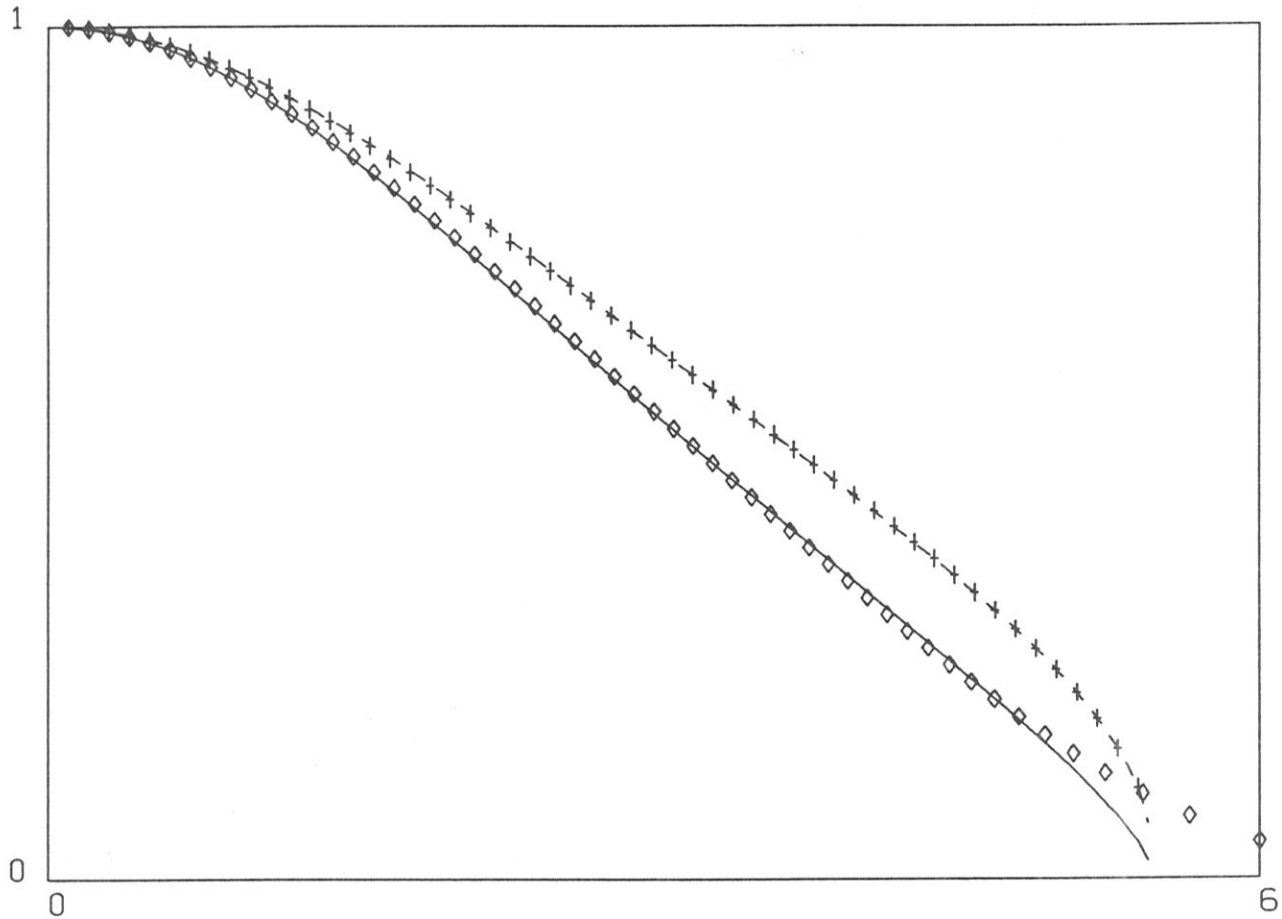

Fig. 4d
Density and temperature vs. r
for $\beta_i = 0.5$
Solid : density , numerical
Dashed: temperature, numerical
Crossed: temperature, acc. to eq.(33)
$T_P = n^{2/3}\, e^{\hat{\alpha} n - \hat{\alpha}}$
Rhombuses: density, acc. to eq.(34)
$r = \sqrt{-n_P^{\epsilon}\, \frac{ln\ n_P}{Q}}$